

Cytotoxic and mutagenic potential of juglone: a comparison of free and nano-encapsulated form

Semiha Erisen¹, Tülin Arasoğlu¹, Banu Mansuroğlu¹, İsmail Kocacaliskan¹, and Serap Derman²

¹ Yildiz Technical University, Faculty of Science and Letters Molecular Biology and Genetics Department, Esenler-Istanbul, Turkey

² Yildiz Technical University, Faculty of Chemical and Metallurgical Engineering, Department of Bioengineering, Istanbul, Turkey

[Received in October 2019; Similarity Check in October 2019; Accepted in February 2020]

Despite its evidenced beneficial herbicidal, antibacterial, antiviral, antifungal, and antioxidant effects, the application of juglone (5-hydroxy-1,4-naphthoquinone) is limited due to its low water solubility and allelopathic and toxic effects. In recent years, research has aimed to overcome these limitations by increasing its solubility and controlling its release through nanoparticulate systems. This is the first study to have synthesised and characterised juglone-loaded polymeric nanoparticles and compared them with free juglone for cytotoxicity in mouse (L929 fibroblasts) and alfalfa cells and for mutagenic potential in *Salmonella typhimurium* TA98/100. Mouse and plant cells treated with free and nano-encapsulated juglone showed a decrease in cell viability in a dose and time-dependent manner, but this effect was significantly lower with the nano-encapsulated form at lower doses. In the TA98 strain with S9, nano-encapsulated juglone did not exhibit mutagenic effects, unlike the free form. Since all results show that juglone encapsulation with polymeric nanoparticles reduced the toxic and mutagenic effects, it has a promising potential to be applied in medicine, food safety, and agriculture.

KEY WORDS: alfalfa; L929 fibroblasts; nanoparticle; PLGA; *S. typhimurium*

Walnut preparations are used in traditional medicine for the treatment of many health problems such as fungal, bacterial, viral, and helminthic infections, hypotension, hypoglycaemia, and even cancer (1). Walnut has the highest concentrations of an allelochemical molecule which is an amber pigment largely responsible for its biological activity (Figure 1) (2). Juglone is found in the root, leaves, bark, and nuts of several walnut species of the *Juglandaceae* family, including *Juglans nigra*, *Juglans regia*, *Juglans cinerea*, and *Carya illinoensis* (3). Even though it is poorly soluble in water, juglone will adversely affect plants growing around the tree (2, 4). In terms of its toxicity mechanisms, a number of studies have established that it causes cell death, disrupts the cell cycle, modifies DNA (especially in rapidly dividing cells), inhibits mRNA synthesis, alkylates basic protein thiol or amine groups, and reduces tumour suppressor levels (2, 5–7).

Nowadays, new antibiotics are needed to address increasing antimicrobial resistance, but their development and approval cannot keep up the pace with this issue (8). It is therefore essential to develop new antibacterials with different bacterial killing mechanisms than those of conventional antibiotics. Considering its high antimicrobial effect against infections, juglone bears a promise in this

respect. It has already been evidenced for herbicidal (9), antibacterial (10–13), antiviral (14), antifungal (15, 16), antioxidant (13), antiparasitic (17), and anticancer (18–20) properties. However, its hydrophobic structure and high toxicity limit its application in biological systems (2, 4).

A promising strategy to overcome this limitation of juglone and many other materials comes with nanosized drug delivery systems, which have attracted considerable interest in recent years (21, 22). Nanoparticulate systems provide greater biocompatibility and bioavailability and lower the doses of active substances, still achieving the desired effect through controlled release (23, 24). This is particularly true for polymeric nanoparticles such as the poly (D,L-lactic-co-glycolic acid) (PLGA) polymer, as it increases biocompatibility and therapeutic index of active ingredients (Figure 1) (22). Biodegradation of PLGA does not lead to toxicity. Lactic acid from hydrolysis products enters the tricarboxylic acid cycle and is excreted as carbon dioxide and water. Glycolic acid is likewise metabolised to carbon dioxide and water or directly excreted from the kidneys (25).

The aim of this study was therefore to compare cytotoxic and mutagenic properties of juglone-loaded polymeric nanoparticles (JNPs) with those of free juglone. For this purpose, we encapsulated juglone in PLGA nanoparticles, and characterised their physicochemical and release profile. Then, for the first time in literature, we compared the cytotoxic activity of JNPs with juglone in plant cell (alfalfa)

Corresponding author: Tülin Arasoğlu, Yildiz Technical University, Faculty of Science and Letters, Molecular Biology and Genetics Department, 34220, Esenler-Istanbul/Turkey, E-mail: ozbektulin@gmail.com

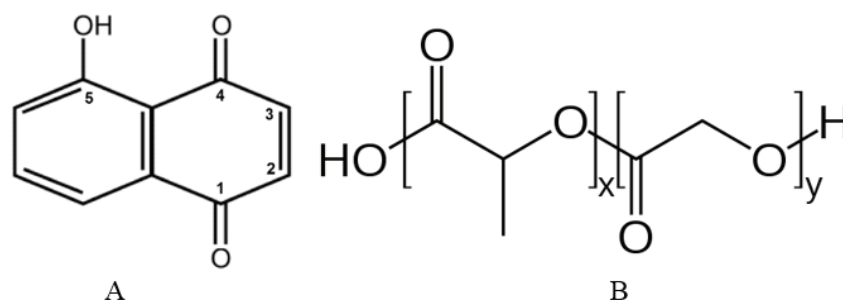


Figure 1 Chemical structure of juglone (A) and poly (lactic-co-glycolic acid) (B)

and mouse cell culture (L929 fibroblast cells). Additionally, we investigated their mutagenic potential in *Salmonella typhimurium* strains TA98 and TA100 in culture media with or without the S9 metabolic activation system.

MATERIALS AND METHODS

Materials

Juglone (Mw: 174.15 g/mol, CAS Number: 481-39-0), polyvinyl alcohol (PVA, Mw 31–50 kDa, 87–89 % hydrolyzed, CAS Number: 9002-89-5), PLGA (50:50 lactide:glycolide; inherent viscosity 0.45–0.60 dL/g, Mw ~38–54 kDa, CAS Number: 26780-50-7), and dichloromethane (DCM, CAS Number: 75-09-2) were purchased from Sigma-Aldrich (St. Louis, MO, USA).

Plant suspension cultures were established from alfalfa (*Medicago sativa* cv Verco) seeds kindly provided by Dr Satı Uzun (University of Erziyes, Turkey). 2,4-dichlorophenoxyacetic acid, kinetin, sucrose, and agar used for preparing the Murashige and Skoog (MS) medium were purchased from Sigma-Aldrich.

The mouse fibroblast cell line L929 was obtained from the American Type Culture Collection (ATCC, Manassas, VA, USA). Dulbecco's modified Eagle's medium (DMEM) / Ham's Nutrient Mixture F-12 medium, foetal bovine serum (FBS), penicillin, and L-glutamine used in the preparation of fibroblast cell cultures were purchased from Sigma-Aldrich. The Ames Microplate Format Mutagenicity Assay™ 98/100 kit and strains were provided from Anaria-Xenometrix (Mason, OH, USA). All the chemicals and solvents used for mutagenicity study were of analytical grade. Ultra-pure water was obtained from the Millipore MilliQ Gradient system (Merck Millipore, Burlington, MA, USA).

Nanoparticle synthesis and characterisation

Juglone-loaded nanoparticles (JNPs) were synthesised using the single-emulsion solvent evaporation method described in our previous study (16) with minor modifications. 20 mg of juglone and 100 mg of PLGA were first dissolved in 3.5 mL DCM and stirred to ensure that all materials were dissolved. The obtained organic phase was

added dropwise to 8 mL of aqueous PVA solution (3 % w/v) over an ice bath, and the mixture was sonicated with a microtip probe sonicator (HD3100, Bandelin, Berlin, Germany, output power 100 W) at 80 % power for 2 min. The obtained oil-in-water (o/w) emulsion was then diluted in 35 mL of PVA solution (0.1 % w/v) and mixed on a magnetic stirrer at room temperature overnight for the organic solvent to evaporate. The obtained nanoparticles were centrifuged at 10,000xg for 40 min (Beckman Coulter, Allegra-X-30R) and washed three times with ultrapure water. After that, the suspensions were lyophilised and solid nanoparticles stored at -80 °C until use.

Encapsulation efficiency and drug loading were determined by indirect quantification using UV-vis spectroscopy (UV 1800, Shimadzu, Tokyo, Japan). UV absorbance of the supernatant was analysed at 424 nm in triplicate. Juglone concentration was calculated using a previously constructed standard calibration curve (26). Encapsulation efficiency (EE) and drug loading (DL) of juglone were calculated as follows:

$$EE\% = \frac{\text{Encapsulated juglone in NPs (mg)}}{\text{Encapsulated juglone amount (mg)}} \quad [1]$$

$$DL\% = \frac{\text{Encapsulated juglone in NPs (mg)}}{\text{Obtained nanoparticle amount (mg)}} \times 100 \quad [2]$$

The mean diameter, particle size distribution, zeta potential (ζ), and polydispersity index (PDI) of the nanoparticles were investigated by photon correlation spectroscopy using a Zetasizer Nano ZS (Malvern, UK) instrument (27). Nanoparticles were also inspected for shape and surface morphology with scanning electron microscopy (SEM, A JSM-7001FA, Jeol, Japan) as previously described in our studies (10), with an acceleration voltage of 10–30 kV. Successful encapsulation of juglone was evidenced with Fourier-transform infrared spectroscopy (FT-IR) using an IR-Prestige 21 FT-IR spectrophotometer (Shimadzu, Kyoto, Japan) in ATR mode. The FT-IR spectra ranging between 600 and 4000 cm^{-1} were obtained with resolution of 4 cm^{-1} (28).

Juglone release was established with a modified dissolution method in triplicate, in which 5 mg of nanoparticles were suspended in 2 mL of phosphate buffer saline (PBS) and incubated 37 °C in a shaking incubator (150 rpm) at pH of 7.2 (16). The suspensions were

centrifuged and the obtained precipitates, resuspended with 2 mL of fresh PBS, and supernatants analysed with UV-vis spectroscopy at 424 nm. The amount of released juglone was calculated using a previously constructed calibration curve (26).

Fibroblast cell cytotoxicity evaluation

L929 fibroblast cell lines were grown at 37 °C in DMEM/Ham's Nutrient Mixture F-12 medium (1:1) supplemented with 10 % FBS, 100 µg/mL streptomycin, 100 units/mL penicillin, and 0.2 mmol/L L-glutamine in an atmosphere of 95 % air and 5 % CO₂. The medium was changed every two days. The morphology of the cells was examined with an Olympus phase contrast microscope (Olympus CKX41, Tokyo, Japan) at 5x magnification.

The cytotoxic potential of juglone was quantified with the MTT assay (3-(4,5-dimethylthiazol-2-yl)-2,5-diphenyltetrazolium bromide) (29) following the ISO 10993-5 procedure (30). Briefly, 5×10³ fibroblast cells per well were seeded in 96-well plates and incubated at 37 °C for 24 h and then exposed to free and nano-encapsulated juglone in concentrations of 5, 27, 83, 160, 250, 500, and 1000 µmol/L suspended in DMEM/ Ham's Nutrient Mixture F-12 medium (1:1). Following 24- and 48-hour incubation, the supernatant from each well was replaced with fresh MTT reagent in the final concentration of 50 µg/mL of medium. The cells were then incubated at 37 °C for 3 h, and their viability determined by measuring absorbance at 570 nm in a universal microplate reader. Control growth was considered to be 100 % viable. Metabolic activity was expressed as mean±SD. Cell viability (%) was calculated as follows:

$$\text{Cell viability (\%)} = \frac{\text{OD value of treated cells}}{\text{OD value of untreated cells (control)}} \times 100 \quad [3]$$

Alfalfa cell cytotoxicity evaluation

Leaf explants (5–6 cm) removed from *in vitro* aseptic seedling of alfalfa were cultured on MS medium supplemented with 3 mg/L 2,4-dichlorophenoxyacetic acid, 0.5 mg/L kinetin, 3 % (w/v) sucrose, and 0.8 % (w/v) agar for callusing. The pH of the medium was adjusted to 5.6 before autoclaving at 121 °C for 20 min. After six weeks, cell suspension cultures were initiated in 150 mL Erlenmeyer flasks with 1 g of friable callus in 50 mL of MS liquid medium containing plant growth regulator used for the callus phase. The cultures were kept in a dark growth chamber at 24±2 °C under continuous agitation of 110 rpm in an orbital shaker. After 21 days, 30 mL of fresh medium was added to 10 mL of decanted suspension culture, and the suspensions were subcultured every 10 days by transferring 10–30 mL of fresh medium. Cell density was determined as ~1.5×10⁵ cells /mL using the Thoma cell counting chamber. These cultures were used as stock.

Alfalfa cells were exposed to the same free and nano-encapsulated juglone concentrations as the mouse cells. 100 µL free or nano-encapsulated juglone solutions were added

to 4 mL of 5–6 day old alfalfa suspension cultures under continuous agitation at 110 rpm in an orbital shaker. After 24 and 48 h of incubation, cell suspensions (1 mL) were transferred to tubes and centrifuged at 445xg for 5 min to collect the cells. Cell viability was determined with the MTT assay with minor modifications (31). 100 µL of a 5 mg/mL MTT solution was added to each tube and incubated in dark on a shaker at 24 °C for 2 h. The pellet was removed by centrifugation at 1000xg for 5 min and resuspended with 200 µL of DMSO for 10 min. The supernatant was placed on microplate and analysed at 570 nm in a universal microplate reader. Cell viability (%) was calculated as follows:

$$\text{Cell viability (\%)} = \frac{\text{OD value of treated cells}}{\text{OD value of untreated cells (control)}} \times 100 \quad [4]$$

Bacterial cell mutagenicity and cytotoxicity evaluation

To determine juglone mutagenicity we chose the Ames MPF assay as a method that shows reverse mutagenicity in *Salmonella typhimurium* strains TA98 and TA100. These strains cannot grow in histidine-free media, since they have lost the ability to produce histidine due to point mutations (either frame-shift for TA98 or base-pair for TA100) in the histidine (His) operon. However, a new mutation in this operon (such as the one caused by juglone) reverts His auxotroph into a prototroph and reverts the initial mutation so that the strains can now grow in histidine-free media. Frozen stock cultures of *S. typhimurium* TA98 and TA100 strains in histidine-free medium were thawed at room temperature and pipetted to be completely homogenised. They were prepared by incubating in tubes containing 10 mL growth medium and 10 µL ampicillin (50 mg/mL) at 37 °C and shaking at 200 rpm for 16–18 h overnight. When the cultures reached spectrophotometric OD₆₀₀ ≥ 2.0, they were ready for mutagenicity testing.

The mutagenic activity of free and nano-encapsulated juglone was determined with the Ames MPF™ 98/100 bacterial reverse mutation assay (Anaria-Xenometrix, Mason, OH, USA) with or without the metabolic activation of the rat liver S9 microsomal fraction. The study was carried out in accordance with the kit protocol (32). 2-nitrofluorene (2NF; 2 µg/mL), 4-nitroquinalone-*N*-oxide (4NQO; 0.1 µg/mL), and 2-aminoanthracene (2-AA; 2.5 µg/mL for TA100, 1.0 µg/mL for TA98) were used as positive control (mutagens). Water (solvent) was used as negative control. The S9 metabolic activation system was prepared as a 30 % mix of S9 fraction and cofactors (32–34). Free and nano-encapsulated juglone stock concentrations were set to contain 5.7 mmol/L juglone. The final concentration of juglone applied to all wells ranged between 0.31 and 10 µmol/L. Bacterial cultures in a 24-well plate were exposed to 10 µL of free or nano-encapsulated juglone stock solution for 90 min (37 °C, 250 rpm). The liquid exposure medium contained trace amounts of required histidine. In the presence of S9, the volume of the exposure medium was reduced as indicated in the kit to produce a 240 µL mix

of S9 and exposure medium containing bacterial culture. This mix was added to the wells containing juglone solutions, resulting in a total volume of 250 μL . At the end of exposure, each well of the 24-well plates received 2.6 mL of histidine-free indicator medium. 50 μL of the culture in each well was taken and distributed to a 384-well plate. After 48 h of incubation at 37 $^{\circ}\text{C}$, the metabolism of prototroph cells that succeeded to reproduce in histidine-free medium lowers the pH of the substrate, causing a change in colour from purple (bromoresol) to yellow as a result of the catabolic activity of the revertant bacteria. This colour is interpreted as a mutagenic effect, and each well is scored for either yellow (mutagenic effect or positive control) or purple (no-mutagenic effect or solvent control) (32, 34, 35).

Juglone cytotoxicity to the *S. typhimurium* TA98 and 100 strains was investigated as described in the “pre-screen determination of dose range” section of the kit protocol (32). Only free juglone was evaluated, because we did not expect any problem with the solubility of the PLGA nanoparticle system, from which juglone is slowly released. The kit protocol recommends the use of 25 times higher stock sample concentrations than the highest concentration to be used in the mutagenicity study. However, as juglone water solubility is very low, we adjusted its concentration range from 2.5 to 80 $\mu\text{mol/L}$. Briefly, bacterial overnight cultures were incubated in exposure medium at 37 $^{\circ}\text{C}$ for 90 min and measured spectrophotometrically at OD₆₀₀. The results were evaluated according to turbidity and sediment. Being an indication of bacterial lysis, pure image is an indicator of a cytotoxic dose. The well containing a lower dose should be more blurred and have no sediment at the bottom. The highest concentration to be applied in the Ames assay was therefore the lowest sample concentration with the highest solubility and no cytotoxicity.

Statistical analysis

Cytotoxicity results [means of four (mammalian cells) and three (plant cells) independent treatments repeated for all groups, starting with the cell growth step] were analysed with a GraphPad Prism6 software (San Diego, CA, USA). The differences between JNPs and free juglone within each dose were determined using the *t*-test. *P* values <0.05 were considered significant. IC₅₀ values were calculated using Prism6.

The criteria for the evaluation of mutagenicity results (means \pm standard deviations of the number of revertant wells) were the number of positive wells and dose dependency (32, 34, 36). The data were evaluated with the cumulative binomial distribution test according to the manufacturer’s instructions. The increase of revertants relative to the solvent control was determined by dividing the mean number of positive wells (yellow well) at each dose with solvent control baseline, which is obtained by adding one standard deviation to the mean number of

positive wells of the solvent control. A twofold or higher increase over baseline was considered a mutagenic effect. The dose-response relationship and the differences were considered significant when the binomial value was $\geq 99\%$ (21).

RESULTS AND DISCUSSION

Table 1 shows the physicochemical properties of JNPs. In terms of encapsulation efficiency and drug loading activities our results are compatible with similar reports in the literature (37–39).

JNPs had a narrow size distribution (Figure 2A), and were quite spherical, smooth, and homogeneous in size (Figure 2B SEM image).

Figure 2C compares the FT-IR absorbance spectra of free juglone, JNPs, and juglone-free PLGA nanoparticles. Juglone exhibited the main characteristic triple peaks at 1593 cm^{-1} ($\text{C}_2=\text{C}_3$), 1635 cm^{-1} ($\text{C}_4=\text{O}$), and 1662 cm^{-1} ($\text{C}_1=\text{O}$), while the peak at 1288 cm^{-1} corresponds to the C_5-O group. Unlike juglone, both PLGA and JNPs have a carbonyl group absorbance band at 1751 cm^{-1} . A comparison of all three spectra clearly shows a similarity between JNPs and PLGA, and the absence of juglone’s specific peak in the JNPs spectrum indicates that juglone was successfully coated with the PLGA nanoparticles.

Juglone cumulative release from the nanoparticles in phosphate buffer saline at pH 7.4 shows a triphasic pattern of up to 30 days (Figure 2D). It starts with 28.62 \pm 2.3 % at the end of the first hour, then soars to 56.53 \pm 2.5 % at the end of hour 24, and peaks to 88.86 \pm 2.8 % at the end of day 9. After that, it slows down to finally reach 92.72 \pm 4.1 % at the end of day 30.

Juglone/JNP effect on fibroblast cell viability

Figure 3 shows the inhibitory effects of juglone and JNPs on L929 fibroblast cell viability (measured with the MTT assay). In the first 24 h, juglone and JNP had a similar cytotoxic effect, with half-maximal inhibitory concentrations (IC₅₀) of 290 and 330 $\mu\text{mol/L}$, respectively (Figure 3A). After 48 h, free juglone toxicity became far more prominent, with IC₅₀ of 60 $\mu\text{mol/L}$, as opposed to 270 $\mu\text{mol/L}$ for JNPs (Figure 3B). Cell viability drastically dropped at juglone concentrations of 83 $\mu\text{mol/L}$ (*p*=0.038), 160 $\mu\text{mol/L}$ (*p*=0.013), and 250 $\mu\text{mol/L}$ (*p*=0.034) compared to JNPs. In a study by Ramirez et al. (40), high cytotoxic activity of synthetic juglone and its derivatives on L929 fibroblast cells began at the lowest concentration (5.3 $\mu\text{mol/L}$) applied. Cytotoxic activity this high might be advantageous for cancer cell lines, but is unwelcome in other therapeutic applications. Significantly lower cytotoxic effect of JNPs is therefore an advantage here, most likely thanks to low and sustained release from the nanosystem. This is in line with reports that biodegradable nanoparticles used as drug

Table 1 Physicochemical properties of juglone loaded PLGA nanoparticles

Encapsulating efficiency (%)	Drug loading (%)	Particle size (nm)	Zeta potential (mV)	Polydispersity index
29.95±2.8	15.42±2.1	213.33±5.2	-14.58±2.8	0.115±0.03

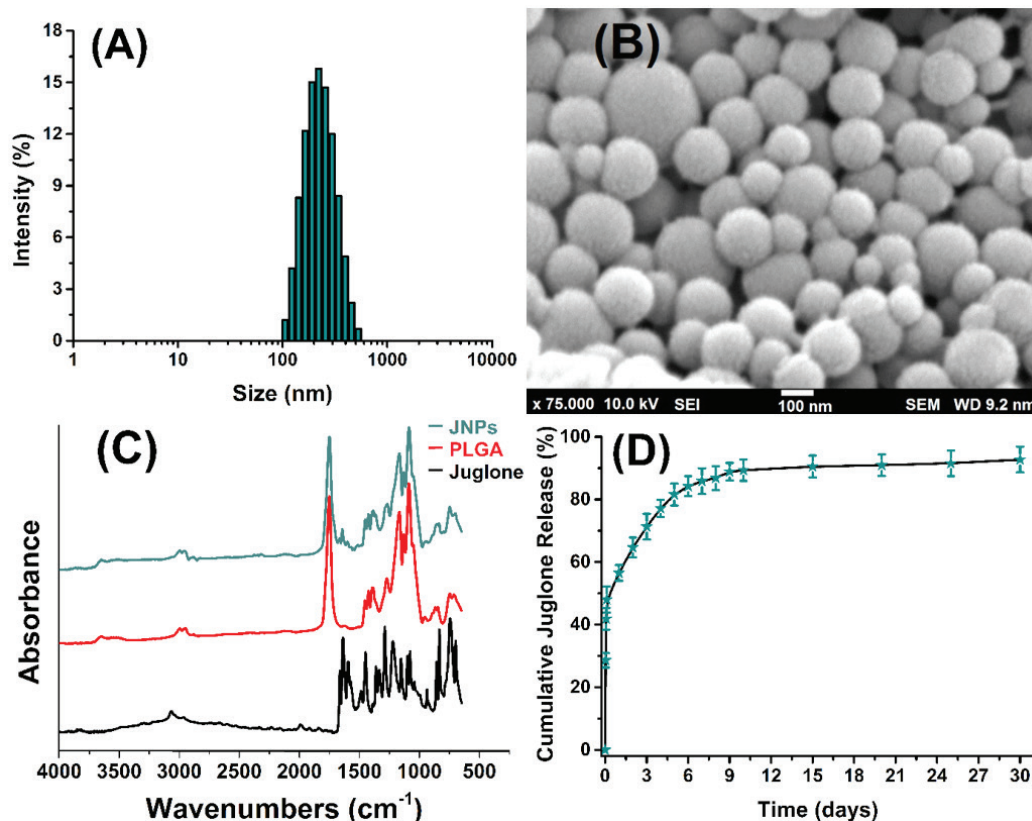


Figure 2 Particle size distribution (A), scanning electron microscopy image (B), FT-IR spectra (C), and release pattern (D) of nanoparticles

carriers protect substances from degradation and reduce their toxicity or side effects (41).

Juglone/JNP effect on alfalfa cell viability

Similar to the fibroblast cells, the cytotoxicity of either free or nano-encapsulated juglone in alfalfa cells was dose-dependent and was not significant at doses lower than 27 and 83 $\mu\text{mol/L}$, respectively. Similar was reported by other studies for alfalfa and other plants (42–47).

Free and nano-encapsulated juglone did not significantly differ in their effect on cell viability in the first 24 h either (Figure 4A), with respective IC_{50} of 316 and 382 $\mu\text{mol/L}$. After 48 h, however, free juglone doses of 5 and 27 $\mu\text{mol/L}$ had a significantly higher cytotoxic effect (Figure 4B). The respective IC_{50} dropped to 2 $\mu\text{mol/L}$ for juglone and 70 $\mu\text{mol/L}$ for JNPs.

Ames test findings

According to the spectrophotometric measurements and turbidimetric observation (OD_{600}), the juglone dose of 10 $\mu\text{mol/L}$ was selected as the highest non-cytotoxic concentration applied in the Ames test. Figures 5 and 6 show the results for *S. typhimurium* TA98 and 100 strains

in the absence (-S9) and presence (+S9) of metabolic activation. Juglone showed mutagenic activity at 2.5 and 1.25 $\mu\text{mol/L}$ on TA98 strain with S9 metabolic activation system but not on TA100 with or without S9. Juglone also significantly increased the number of revertant wells at the concentration of 0.62 $\mu\text{mol/L}$ in the TA98 strain without the S9 medium (B value ≥ 0.99), but this increase was not considered mutagenic, because it still was not twice the baseline.

Our results indicate that juglone causes frameshift mutations which may be related to hydroxyl substitution. In the mutagenicity study carried out on natural quinones by Tikkaen et al. (48) hydrocarbons with simple hydroxyl and/or methyl substituents were extremely important for the mutagenic effect, and while juglone showed a mutagenic effect on the TA2637 strain with S9 metabolic activation, the effect was extremely weak in the TA98 strain. These results are consistent with our study. In another study (49), the mutagenic effect of juglone on *S. typhimurium* TA98 in the presence of the S9 metabolic activation system was dose-independent, and, according to the authors, related to the hydroxyl group at position 5. Besides, juglone is biotransformed by liver metabolism and may affect several

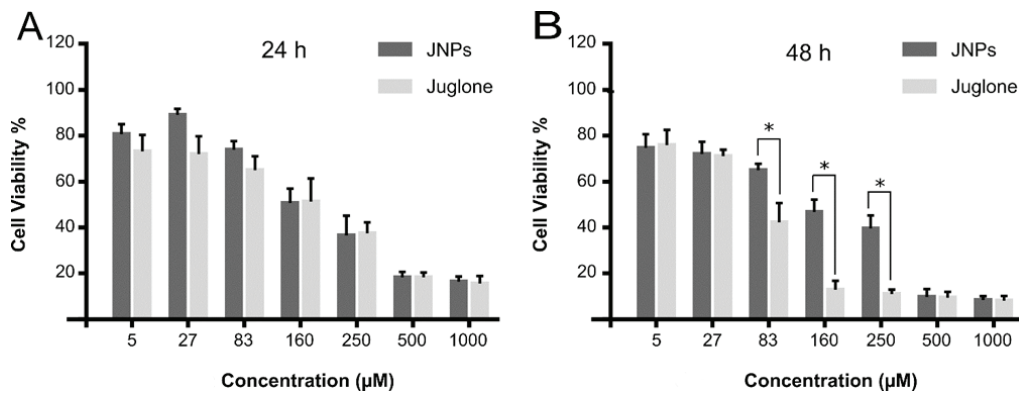


Figure 3 Viability of L929 fibroblasts treated with free and PLGA nanoparticle-coated juglone (JNP) after 24 h (A) and 48 h (B); Cell viability was measured with the MTT assay. Values are expressed as means of quadruple samples with standard error. *statistically significant differences between juglone and JNP ($p < 0.05$)

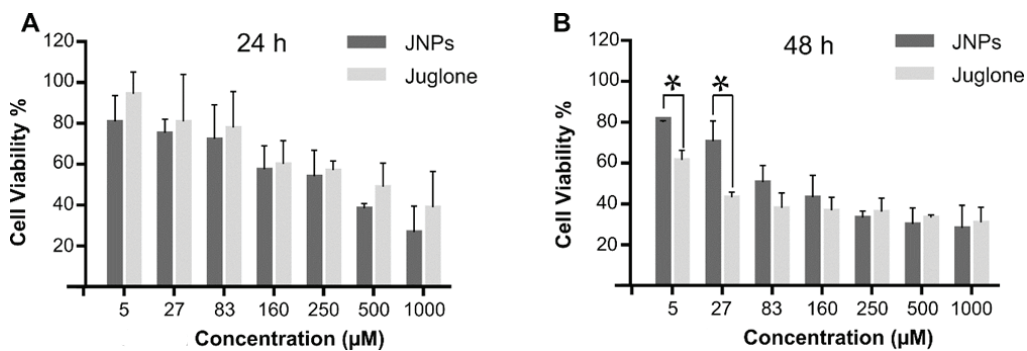


Figure 4 Viability of alfalfa cells treated with free and PLGA nanoparticle-coated juglone (JNP) after 24 h (A) and 48 h (B); Cell viability was measured with the MTT assay. Values are expressed as means of triple samples with standard error. *statistically significant differences between juglone and JNP ($p < 0.05$)

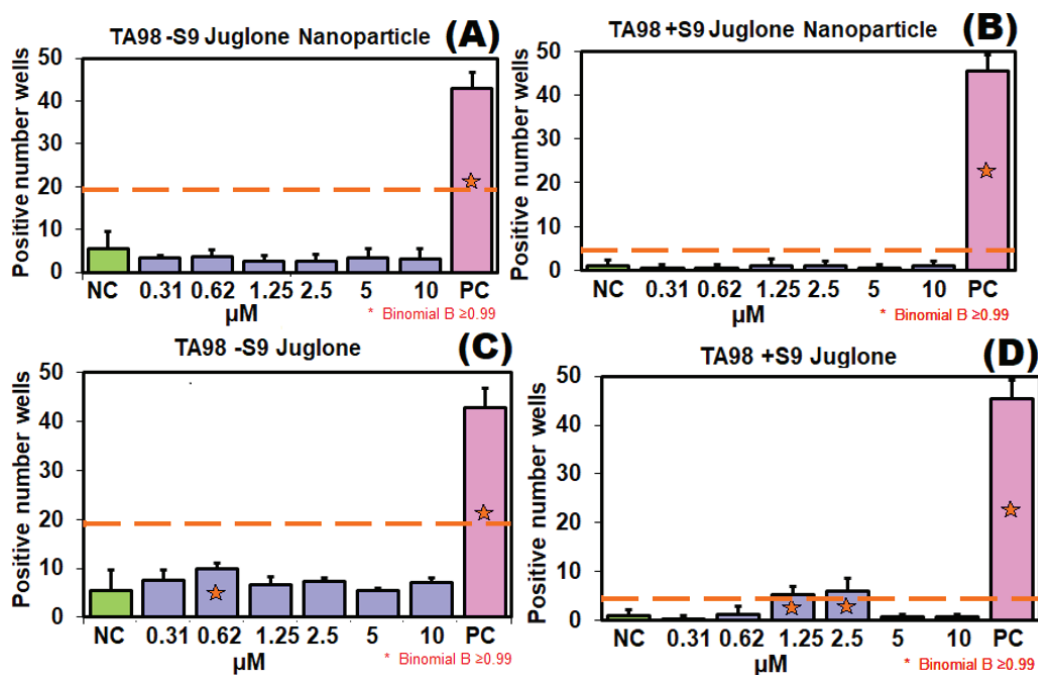


Figure 5 Potential mutagenicity in *S. typhimurium* TA98 treated with 0.31–10 µmol/L juglone: (A) TA98-S9 treated with JNPs; (B) TA98+S9 treated with JNPs; (C) TA98-S9 treated with free juglone; (D) TA98+S9 treated with free juglone; PC – positive control: 2-NF (2 µg/mL) and 4-NQO (0.1 µg/mL) without S9 and 2-AA (1 µg/mL) with S9; NC – negative control: water; *B value ≥ 0.99

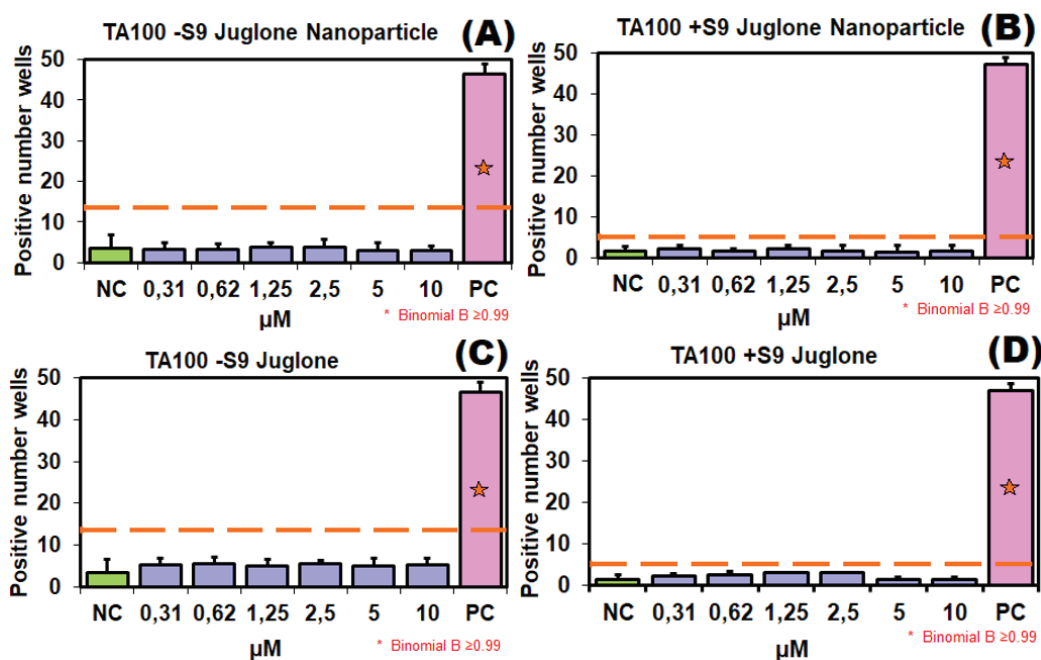


Figure 6 Potential mutagenicity in *S. typhimurium* TA100 treated with 0.31–10 μmol/L juglone: (A) TA100-S9 treated with JNPs; (B) TA100+S9 treated with JNPs; (C) TA100-S9 treated with free juglone; (D) TA100+S9 treated with free juglone; PC – positive control: 2-NF (2 μg/mL) and 4-NQO (0.1 μg/mL) without S9 and 2-AA (2.5 μg/mL) with S9; NC – negative control: water; *B value ≥ 0.99

metabolic pathways that are somehow linked to energy metabolism. Saling et al. (17) observed that at low concentrations juglone stimulated oxygen consumption, lowered ATP content, increased the NADH/NAD⁺ ratio, and inhibited gluconeogenesis, whereas at high concentrations it triggered ATP production, hyperthermia, and even death. In the light of these findings, when S9 is added to a juglone-containing environment, products resulting from biotransformation by liver enzymes cause frameshift mutations in the TA98 strain. S9 is a liver extract containing active liver enzymes (P450 activity) which simulate hepatic metabolism in *in vitro* experiments (e.g., rat, hamster, or human) (17). In contrast, JNPs did not show mutagenic activity (Figure 5 and 6), probably because of the sustained and lower release of juglone as PLGA nanoparticles degrade. This elimination of mutagenic activity is important in terms of genotoxicity, as there is little information about the mutagenicity of pharmaceutical products using PLGA as carrier. Kruci et al. (50), for instance, found no mutagenic activity of PLGA/PHB fibrous nanocomposite implants. Similarly, anticancer drugs encapsulated in PLGA had toxicity compared to their free-form counterparts (51). This suggests that JNPs reduce genotoxicity and cytotoxicity through similar mechanisms.

CONCLUSION

Our findings have confirmed both the mutagenic and cytotoxic effects of free juglone, reported in literature. Compared to free juglone, the toxicity of PLGA nanoparticle-coated juglone was reduced at low doses due to controlled release properties. Furthermore, the nanoparticle system

showed no mutagenicity and improved the biocompatibility of juglone, retaining at the same time the beneficial action of natural juglone.

Our findings provide important information about possible applications of the investigated JNPs. Their IC₅₀ values were significantly higher than the toxic dose for the mutant *Salmonella* bacteria, which suggests that nanoparticle-coated juglone can kill prokaryotic cells without damaging eukaryotic cells. In other words, this system can be used in pharmaceutical fungicidal and bactericidal applications, which remains to be verified by future *in vitro* human cell line studies and *in vivo* animal experiments. Our findings also suggest that nanoparticle-coated juglone could be used in food safety applications and agriculture.

Funding

This research has not been supported by any organisation.

Conflict of interest

None to declare.

REFERENCES

1. Aithal BK, Kumar MR, Rao BN, Udupa N, Rao BS. Juglone, a naphthoquinone from walnut, exerts cytotoxic and genotoxic effects against cultured melanoma tumor cells. *Cell Biol Int* 2009;33:1039–49. doi: 10.1016/j.cellbi.2009.06.018
2. Coder KD. Black Walnut Allelopathy: Tree Chemical Warfare. *Allelopathy Series*. 2011;WSFN11–10:1–13.

3. Lee K-C. Nature and occurrence of juglone in *Juglans nigra* L [master of science]. Manhattan, Kansas: Kansas State University, Department of Horticulture; 1967.
4. Kocacaliskan I, Terzi I. Allelopathic effects of walnut leaf extracts and juglone on seed germination and seedling growth. *J Hort Sci Biotechnol* 2001;76:436–40. doi: 10.1080/14620316.2001.11511390
5. Paulsen MT, Ljungman M. The natural toxin juglone causes degradation of p53 and induces rapid H2AX phosphorylation and cell death in human fibroblasts. *Toxicol Appl Pharmacol* 2005;209:1–9. doi: 10.1016/j.taap.2005.03.005
6. Hejl AM, Koster KL. Juglone disrupts root plasma membrane H⁺-ATPase activity and impairs water uptake, root respiration, and growth in soybean (*Glycine max*) and corn (*Zea mays*). *J Chem Ecol* 2004;30:453–71. doi: 10.1023/b:joec.0000017988.20530.d5
7. Inbaraj JJ, Chignell CF. Cytotoxic action of juglone and plumbagin: a mechanistic study using HaCaT keratinocytes. *Chem Res Toxicol* 2004;17:55–62. doi: 10.1021/tx034132s
8. Esterbauer H, Cheeseman KH. Determination of aldehydic lipid peroxidation products: Malonaldehyde and 4-hydroxynonenal. *Methods Enzymol* 1990;186:407–21. doi: 10.1016/0076-6879(90)86134-h
9. Dama L, Poul B, Jadhav B. Antimicrobial activity of naphthoquinonic compounds. *J Ecotoxicol Environ Monit* 1998;8:213–5.
10. Arasoğlu T, Derman S, Mansuroğlu B, Uzunoglu D, Koçyiğit BS, Gümüş B, Acar T, Tuncer B. Preparation, characterization, and enhanced antimicrobial activity: quercetin-loaded PLGA nanoparticles against foodborne pathogens. *Turk J Biol* 2017;41:127–40. doi: 10.3906/biy-1604-80
11. Tan DTC, Osman H, Mohamad S, Kamaruddin AH. Synthesis and antibacterial activity of juglone derivatives. *J Chem Chem Engin* 2012;6:84–9.
12. Xu H, Yu X, Qu S, Sui D. Juglone, isolated from *Juglans mandshurica Maxim*, induces apoptosis via down-regulation of AR expression in human prostate cancer LNCaP cells. *Bioorg Med Chem Lett* 2013;23:3631–4. doi: 10.1016/j.bmcl.2013.04.007
13. Zakavi F, Golpasand Hagh L, Daraeighadikolaei A, Farajzadeh Sheikh A, Daraeighadikolaei A, Leilavi Shooshtari Z. Antibacterial effect of *Juglans regia* bark against oral pathologic bacteria. *Int J Dent* 2013;2013:854765. doi: 10.1155/2013/854765
14. Montenegro RC, Araújo AJ, Molina MT, Marinho Filho JDB, Rocha DD, López-Montero E, Goulart MO, Bento E, Alves APNN, Pessoa C, de Moraes MO, Costa-Lotufo LV. Cytotoxic activity of naphthoquinones with special emphasis on juglone and its 5-O-methyl derivative. *Chem Biol Interact* 2010;184:439–48. doi: 10.1016/j.cbi.2010.01.041
15. Shahidi Bonjar G, Aghighi S, Karimi Nik A. Antibacterial and antifungal survey in plants used in indigenous herbal-medicine of south east regions of Iran. *J Biol Sci* 2004;4:405–12. doi: 10.3923/jbs.2004.405.412
16. Arasoglu T, Mansuroglu B, Derman S, Gumus B, Kocyiğit B, Acar T, Kocacaliskan I. Enhancement of antifungal activity of juglone (5-Hydroxy-1,4-naphthoquinone) using a Poly(D,L-lactic-co-glycolic acid) (PLGA) nanoparticle system. *J Agric Food Chem* 2016;64:7087–94. doi: 10.1021/acs.jafc.6b03309
17. Saling SC, Comar JF, Mito MS, Peralta RM, Bracht A. Actions of juglone on energy metabolism in the rat liver. *Toxicol Appl Pharmacol* 2011;257:319–27. doi: 10.1016/j.taap.2011.09.004
18. Aithal KB, Kumar SM, Rao NB, Udupa N, Rao SB. Juglone, a naphthoquinone from walnut, exerts cytotoxic and genotoxic effects against cultured melanoma tumor cells. *Cell Biol Int* 2009;33:1039–49. doi: 10.1016/j.cellbi.2009.06.018
19. Strugstad M, Despotovski S. A summary of extraction, synthesis, properties, and potential uses of juglone: A literature review. *J Ecosyst Management* 2013;13(3):1–16.
20. Aithal KB, Kumar S, Rao BN, Udupa N, Rao SBS. Tumor growth inhibitory effect of juglone and its radiation sensitizing potential: *in vivo* and *in vitro* studies. *Integr Cancer Ther* 2012;11:68–80. doi: 10.1177/1534735411403477
21. Abdollahi S, Lotfipour F. PLGA- and PLA-based polymeric nanoparticles for antimicrobial drug delivery. *Biomed Int* 2012;3:1–11.
22. Dinarvand R, Sepehri N, Manoochehri S, Rouhani H, Atyabi F. Polylactide-co-glycolide nanoparticles for controlled delivery of anticancer agents. *Int J Nanomedicine* 2011;6:877–95. doi: 10.2147/IJN.S18905
23. Esmaeili F, Hosseini-Nasr M, Rad-Malekshahi M, Samadi N, Atyabi F, Dinarvand R. Preparation and antibacterial activity evaluation of rifampicin-loaded poly lactide-co-glycolide nanoparticles. *Nanomedicine* 2007;3:161–7. doi: 10.1016/j.nano.2007.03.003
24. Cheow WS, Chang MW, Hadinoto K. Antibacterial efficacy of inhalable levofloxacin-loaded polymeric nanoparticles against *E. coli* biofilm cells: the effect of antibiotic release profile. *Pharmaceut Res* 2010;27:1597–609. doi: 10.1007/s11095-010-0142-6
25. Kerimoglu O, Alarcin E. Poly(lactic-co-glycolic acid) based drug delivery devices for tissue engineering and regenerative medicine. *ANKEM Derg* 2012;26:86–98. doi: 10.5222/ankem.2012.086
26. Arasoglu T, Derman S, Mansuroglu B, Yelkenci G, Kocyiğit B, Gumus B, Acar T, Kocacaliskan I. Synthesis, characterization and antibacterial activity of juglone encapsulated PLGA nanoparticles. *J Appl Microbiol* 2017;123:1407–19. doi: 10.1111/jam.13601
27. Derman S. Caffeic acid phenethyl ester loaded PLGA nanoparticles: effect of various process parameters on reaction yield, encapsulation efficiency, and particle size. *J Nanomater* 2015;2015:ID341848. doi: 10.1155/2015/341848
28. Arasoglu T, Derman S, Mansuroglu B. Comparative evaluation of antibacterial activity of caffeic acid phenethyl ester and PLGA nanoparticle formulation by different methods. *Nanotechnology* 2015;27(2):025103. doi: 10.1088/0957-4484/27/2/025103
29. Mosmann T. Rapid colorimetric assay for cellular growth and survival: application to proliferation and cytotoxicity assays. *J Immunol Methods* 1983;65:55–63. doi: 10.1016/0022-1759(83)90303-4
30. Wallin RF, Arscott E. A practical guide to ISO 10993-5: Cytotoxicity, 1998 [displayed on 29 November 2019]. Available at https://www.namsa.com/wp-content/uploads/2015/10/A-Practical-Guide-to-ISO-10993-5_-Cytotoxicity.pdf
31. Abe K, Matsuki N. Measurement of cellular 3-(4,5-dimethylthiazol-2-yl)-2, 5-diphenyltetrazolium bromide (MTT) reduction activity and lactate dehydrogenase

- release using MTT. *Neurosci Res* 2000;38:325–9. doi: 10.1016/s0168-0102(00)00188-7
32. Xenometrix. Ames MPF™ 98/100 Microplate Format Mutagenicity Assay. Stilwell (CA): Xenometrix; 2015.
33. Hamel A, Roy M, Proudlock R. The bacterial reverse mutation test. In; Proudlock R, editor. Genetic toxicology testing. London: Academic Press Inc.; 2016. p. 79–138.
34. Flückiger-Isler S, Kamber M. Direct comparison of the Ames microplate format (MPF) test in liquid medium with the standard Ames pre-incubation assay on agar plates by use of equivocal to weakly positive test compounds. *Mutat Res* 2012;747:36–45. doi: 10.1016/j.mrgentox.2012.03.014
35. Arasoglu T, Derman S. Assessment of the antigenotoxic activity of Poly(D,L-lactic-co-glycolic acid) nanoparticles loaded with caffeic acid phenethyl ester using the ames *Salmonella*/microsome assay. *J Agric Food Chem* 2018;66:6196–204. doi: 10.1021/acs.jafc.8b01622
36. Escobar P, Kemper R, Tarca J, Nicolette J, Kenyon M, Glowienke S, Sawant S, Christensen J, Johnson T, McKnight C, Ward G, Galloway SM, Custer L, Gocke E, O'Donovan MR, Braun K, Snyder RD, Mahadevan B. Bacterial mutagenicity screening in the pharmaceutical industry. *Mutation Res* 2013;752:99–118. doi: 10.1016/j.mrrev.2012.12.002
37. Dutta D, Paul B, Mukherjee B, Mondal L, Sen S, Chowdhury C, Debnath MC. Nanoencapsulated betulonic acid analogue distinctively improves colorectal carcinoma *in vitro* and *in vivo*. *Sci Rep* 2019;9(1):11506. doi: 10.1038/s41598-019-47743-y
38. Ersoz M, Erdemir A, Duranoglu D, Uzunoglu D, Arasoglu T, Derman S, Mansuroglu B. Comparative evaluation of hesperetin loaded nanoparticles for anticancer activity against C6 glioma cancer cells. *Artif Cells Nanomed Biotechnol* 2019;47:319–29. doi: 10.1080/21691401.2018.1556213
39. Bhattacharya S, Mondal L, Mukherjee B, Dutta L, Ehsan I, Debnath MC, Gaonkar RH, Pal MM, Majumdar S. Apigenin loaded nanoparticle delayed development of hepatocellular carcinoma in rats. *Nanomedicine* 2018;14:1905–17. doi: 10.1016/j.nano.2018.05.011
40. Ramirez O, Motta-Mena LB, Cordova A, Garza KM. A small library of synthetic di-substituted 1,4-naphthoquinones induces ROS-mediated cell death in murine fibroblasts. *PLoS One* 2014;9(9):e106828. doi: 10.1371/journal.pone.0106828
41. Kumari A, Yadav SK, Yadav SC. Biodegradable polymeric nanoparticles based drug delivery systems. *Colloids and Surf B Biointerfaces* 2010;75:1–18. doi: 10.1016/j.colsurfb.2009.09.001
42. Terzi I. Allelopathic effects of juglone and walnut leaf and fruit hull extracts on seed germination and seedling growth in muskmelon and cucumber. *Asian J Chem* 2009;21:1840–6.
43. Kocaçalışkan I, Ceylan M, Terzi I. Effects of juglone on seedling growth in intact and coatless seeds of cucumber (*Cucumis sativus* cv. Beith Alpha). *Sci Res Essays* 2009;4:039–41.
44. Topal S, Kocaçalışkan I, Arslan O, Tel AZ. Herbicidal effects of juglone as an allelochemical. *Phyton* 2007;46:259–69.
45. Terzi I, Kocaçalışkan I, Benlioğlu O, Solak K. Effects of juglone on growth of cucumber seedlings with respect to physiological and anatomical parameters. *Acta Physiol Plant* 2003;25:353–6. doi: 10.1007/s11738-003-0016-1
46. Babula P, Adam V, Havel L, Kizek R. Noteworthy secondary metabolites naphthoquinones-their occurrence, pharmacological properties and analysis. *Curr Pharmaceut Anal* 2009;5:47–68. doi: 10.2174/157341209787314936
47. Babula P, Vaverkova V, Poborilova Z, Ballova L, Masarik M, Provaznik I. Phytotoxic action of naphthoquinone juglone demonstrated on lettuce seedling roots. *Plant Physiol Biochem* 2014;84:78–86. doi: 10.1016/j.plaphy.2014.08.02748
48. Tikkanen L, Matsushima T, Natori S, Yoshihira K. Mutagenicity of natural naphthoquinones and benzoquinones in the *Salmonella*/microsome test. *Mutat Res* 1983;124:25–34. doi: 10.1016/0165-1218(83)90182-9
49. Gaivão I, Sierra LM, Comendador MA. The *w/w*⁺ SMART assay of *Drosophila melanogaster* detects the genotoxic effects of reactive oxygen species inducing compounds. *Mutat Res* 1999;440:139–45. doi: 10.1016/s1383-5718(99)00020-0
50. Krucińska I, Żywicka B, Komisarczyk A, Szymonowicz M, Kowalska S, Zaczyńska E, Struszczyk M, Czarny A, Jadczyk P, Umińska-Wasiluk B. Biological properties of low-toxicity PLGA and PLGA/PHB fibrous nanocomposite implants for osseous tissue regeneration. Part I: Evaluation of potential biotoxicity. *Molecules* 2017;22:p11:E2092. doi: 10.3390/molecules22122092
51. Yoo HS, Lee KH, Oh JE, Park TG. *In vitro* and *in vivo* anti-tumor activities of nanoparticles based on doxorubicin-PLGA conjugates. *J Control Release* 2000;68:419–31. doi: 10.1016/s0168-3659(00)00280-7

Citotoksični i mutageni potencijal juglona u slobodnom i nanoinkapsuliranom obliku

Usprkos dokazanim herbicidnim, protubakterijskim, protuvirusnim, protugljivičnim i antioksidacijskim učincima, primjena juglona (5-hidroksi-1,4-naftokinon) ograničena je zbog njegove slabe topljivosti u vodi te alelopatskoga i toksičnoga djelovanja. Cilj je novijih istraživanja bio ukloniti te prepreke povećanjem njegove topljivosti i boljom regulacijom njegova otpuštanja s pomoću sustava nanočestica. Ovo je, međutim, prvo istraživanje u kojem je sintetiziran i karakteriziran juglon u omotaču polimernih nanočestica te uspoređen sa slobodnim juglonom u smislu citotoksičnosti u mišjih fibroblasta (L929) i biljnih alfalfa stanica te mutagenosti u bakterije *Salmonella typhimurium* TA98 i TA100. Mišje i biljne stanice izložene slobodno u nanoinkapsuliranome juglonu iskazale su smanjenu vijabilnost, koja je ovisila o dozi i vremenu izloženosti, ali je to djelovanje bilo značajno slabije s juglonom u nanočesticama pri nižim dozama. Za razliku od slobodnoga juglona, nanočestice s juglonom nisu djelovale mutageno na *S. typhimurium* soj TA98 s metaboličkim aktivacijskim enzimom S9. Budući da svi rezultati pokazuju kako je inkapsuliranje juglona u polimerne nanočestice smanjilo njegov toksični i mutageni učinak, ovaj oblik ima obećavajući potencijal za primjenu u medicini, poljoprivredi i u području sigurnosti hrane.

KLJUČNE RIJEČI: alfalfa; L929 fibroblasti; nanočestice; PLGA; *S. typhimurium*